Materials and Design 93 (2016) 81–90

Contents lists available at ScienceDirect

Materials and Design

journal homepage: www.elsevier.com/locate/matdes

Comparative study on superplastic tensile behaviors of the as-extruded Ti6Al4V alloys and TiBw/Ti6Al4V composites with tailored architecture

L.J. Huang [a,b,*], C.J. Lu [b], B. Yuan [c], S.L. Wei [b], X.P. Cui [a,b,*], L. Geng [a,b]

[a] State Key Laboratory of Advanced Welding and Joining, Harbin Institute of Technology, P.O. Box 433, Harbin 150001, China
[b] School of Materials Science and Engineering, Harbin Institute of Technology, Harbin 150001, China
[c] Collage of Materials Science and Engineering, Dalian Jiaotong University, Dalian 116028, China

ARTICLE INFO

Article history:
Received 25 November 2015
Received in revised form 24 December 2015
Accepted 29 December 2015
Available online 29 December 2015

Keywords:
Titanium matrix composites
Titanium alloy
Superplasticity
Microstructure evolution
Elongation

ABSTRACT

The superplastic tensile behaviors and mechanisms of Ti6Al4V alloys and TiBw/Ti6Al4V composites with tailored architecture were comparatively studied in order to reveal the superplasticity mechanisms. The superplastic tensile tests were carried out at the temperatures of 900 °C, 925 °C, 950 °C and 975 °C with the strain rate of 0.000316/s, 0.001/s and 0.00316/s, respectively. The composites exhibited higher superplasticity, higher strain rate sensitivity index *m* and lower activation energy Q than the alloys. This might be attributed to the small lamellar aspect ratio and TiBw reinforcement addition. Microstructural observation showed that the aspect ratio of α phase in the Ti6Al4V alloys decreased with increasing strains, and transferred to equiaxed grains only in the tip area. Therefore, necking could not be constrained and transferred to other positions with unfavorable microstructure, led to the needle-like fracture macro morphology. On the contrary, the TiBw/Ti6Al4V composites had weak necking tendency due to the globalization process completed at small strain, which contributed to the large elongations. Recrystallization should be responsible for the decrease in lamellar aspect ratio and increase in volume fraction of β phase, which are considered to be the major coordination mechanism of superplasticity for the as-extruded TiBw/Ti6Al4V composites.

1. Introduction

Titanium matrix composites (TMCs) possess high specific strength, specific stiffness, wear resistance and high temperature durability, which promoted them extensive applications in the field of aerospace, shipping and chemical engineering [1–3]. In the past decades, lots of researches have been concentrated on achieving a homogeneous distribution of reinforcement in the matrix [4,5]. However, the experimental results revealed that the composites with a homogeneous microstructure could only exhibit a limited improvement in strength but at the cost of ductility [6,7]. Recently, Huang et al. [8] has proposed a kind of TMCs with tailored network microstructure. It is surprising to find that the TiBw/Ti6Al4V composites with network microstructure exhibited superior strength and ductility over those with a homogeneous one [9]. Zhang et al. [10] further verified the superiority by designing and fabricating similar inhomogeneous microstructure of TiBw/Ti6Al4V composites.

However, the high cost and poor machinability of the TMCs have restricted their wide applications. In addition, the TMCs components prepared via casting route cannot avoid casting defects like porosity and blowholes. Superplastic deformation (SPD), an economical and near net shape technique and the key solution to solve the above two problems, has become one of the essential processing techniques for the TMCs due to the specific advantages such as reducing material waste, component weight reduction, ability to manufacture special materials and cutting processing cost [11–13].

Many efforts have been made from academic and industries to research the superplastic behaviors, optimize deformation parameters and superplastic properties of the TMCs for establishing the theoretical basis to guide the superplastic deformation process [14,15]. Sinha et al. [16] studied the superplastic deformation behaviors of the 0.1 wt.% B reinforced Ti6Al4V alloys with equiaxed and fine grain microstructure. The results suggested that the optimal deformation temperature of the Ti6Al4V–0.1B composites was 900 °C, which was similar to the conventional Ti6Al4V alloys. In addition, based on the calculation of activation energy and microstructure observation results, grain boundary sliding accompanied by dislocation motion along grain boundaries was the operating deformation mechanism for the composites. Lu et al. [17] carried out superplastic tensile test on the (TiB + TiC)/Ti6Al4V composites with coarse grain size. The maximum elongation of 462% was obtained at 920 °C and 0.001/s for the composites, but much smaller than that of Ti6Al4V alloys with similar microstructure. The decrease in elongation could be attributed to the cavities formed

* Corresponding authors.
E-mail addresses: huanglujun@hit.edu.cn (L.J. Huang), xiping_0725@163.com (X.P. Cui).

http://dx.doi.org/10.1016/j.matdes.2015.12.162
0264-1275/

around the reinforcements in the composites. Finally, the dislocation movement inside α phase was found to be the main accommodation mechanism in superplastic deformation of coarse-grained composite. Huang et al. [18] conducted preliminary research on the superplastic behaviors of the as-sintered TiBw/Ti6Al4V composites with novel network microstructure. It can be observed from the morphology of tensile specimen that the equiaxed network microstructure was drawn into lamina microstructure after superplastic tensile test. What's more, the dynamic recrystallization of Ti6Al4V alloy matrix was found to be an essential coordination mechanism for the composites. However, contrary to the other reports, the novel network distribution of the TiBw reinforcements was considered to be helpful for superplastic deformation process by inhibiting local deformation, decreasing crack propagation rate and refining grain size.

It can be concluded from the above analysis that mechanisms behind the superplastic behavior of the TMCs were still ambiguous. In addition, the composites with inhomogeneous microstructure exhibited a superior combination of strength and ductility compared with the homogeneous composites. Therefore, it is significant to carry out superplastic tensile tests on the TMCs with inhomogeneous microstructure and reveal the deformation mechanisms thereby promoting further applications of TMCs with superior mechanical properties.

Plastic deformation plays a significant role in improving the mechanical properties of TMCs [19]. Among all the plastic deformation techniques, hot extrusion is the most popular one. In addition, the previous studies [8,20,21] have revealed that the tensile strength could be further increased by 13% and the elongation remarkably improved from 3.6% to 6.5% after extrusion, which suggested an excellent combination of strength and ductility of the as-extruded TiBw/Ti6Al4V composites with tailored architecture. Therefore, the present work focuses on the difference of superplastic tensile behaviors and mechanisms between the as-extruded Ti6Al4V alloys and TiBw/Ti6Al4V composites.

2. Experimental procedures

In this study, the TiBw/Ti6Al4V composites with tailored architecture were fabricated according to the quasi-continuous network principle [8]. In addition, to study the effect of TiBw reinforcements during superplastic deformation process, the Ti6Al4V alloys were also prepared by the same methods. Spherical Ti6Al4V powders with a diameter of 150 μm on average and hexagonal-prismatic TiB_2 powders with a size range from 1 to 8 μm were adopted in this study. The morphology of the two raw materials was shown in Fig. 1(a) and (b). Afterwards, in order to make the fine TiB_2 powders adhere onto the surface of large spherical Ti6Al4V powders, low energy ball milling with a speed of 150 r/min for 5 h was carried out. The morphology of Ti6Al4V and mixed Ti–6Al4V–TiB_2 powders after ball milling was shown in Fig. 2(a) and (b), respectively. It can be seen from the SEM images that the morphology of spherical Ti6Al4V remained unchanged and the TiB_2 powders coated onto the surface uniformly after the low energy ball milling. Subsequently, the Ti6Al4V alloys and 3 vol.% TiBw/Ti6Al4V composites were fabricated by reactive hot pressing (RHP) in vacuum at 1200 °C for 1 h with a pressure of 25 MPa. During this process, the TiBw reinforcements were in situ synthesized around the spherical Ti6Al4V powders and formed the network microstructure [22], according to:

$$Ti + TiB_2 \rightarrow 2TiB. \quad (1)$$

Fig. 3 shows the morphology of the as-sintered Ti6Al4V alloys and TiBw/Ti6Al4V composites after RHP. It can be seen from Fig. 3(a) and (b) that the Ti6Al4V alloys had coarse grains with a typical widmanstätten microstructure. The grain size was measured to be 2 mm on average, much larger than that of Ti6Al4V powders, which suggested that no physical interface left after RHP. However, the widmanstätten microstructure formed due to the high temperature combined with a slow cooling speed in furnace was considered to be unfavorable for the strength, ductility and creep resistance of the titanium alloys. The microstructure could be eliminated by followed deformation and heat treatment. Fig. 3(c) and (d) shows the morphologies of TiBw/Ti6Al4V composites fabricated at the same parameters. It is clear that the lamella (similar but not equal to the basketweave) instead of widmanstätten microstructure formed in TiBw/Ti6Al4V composites, which was suggested to be caused by the space restraint from TiBw reinforcements with network microstructure.

The as-sintered Ti6Al4V alloys and TiBw/Ti6Al4V composites were hot extruded at 1100 °C with a ratio of 9 in this study according to the optimized parameters in previous work [8,10]. The superplastic tensile tests were carried out on the as-extruded alloys and composites. The superplastic tensile tests were carried out at the temperature range from 900 °C to 975 °C. The strain rates were decided to be 0.000316/s, 0.001/s and 0.00316/s, respectively. In order to prevent serious oxidation of the tensile specimens at the evaluate temperatures, a layer of glass-ceramic protective coating was covered uniformly on the surface with a melting point of 800 °C and then adhered onto the surface of specimen. After the tensile test, the microstructure and morphology of tensile sample and fracture was characterized using a scanning electron microscopy (SEM, Quanta 200FEG).

3. Results and discussion

3.1. Microstructure observation

The superplastic deformation behavior was found to be sensitive to microstructure, grain size and morphology in particular. Therefore, the microstructure of the as-extruded Ti6Al4V alloys and TiBw/Ti6Al4V

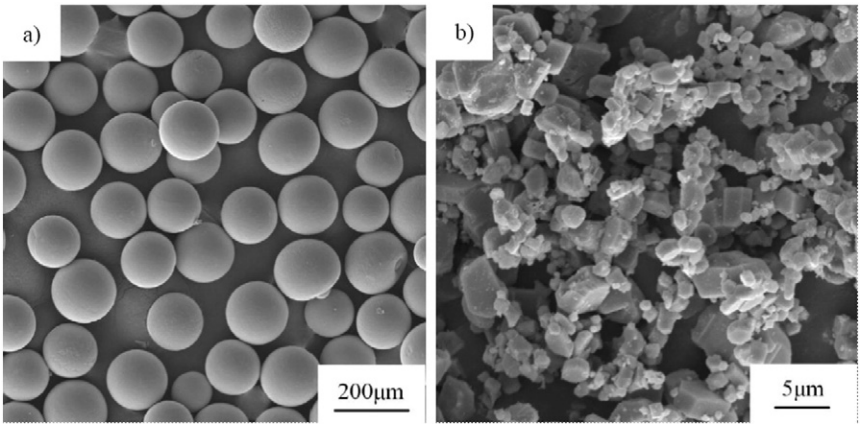

Fig. 1. Morphologies of (a) spherical Ti6Al4V powders and (b) hexagonal-prismatic TiB_2 powders.

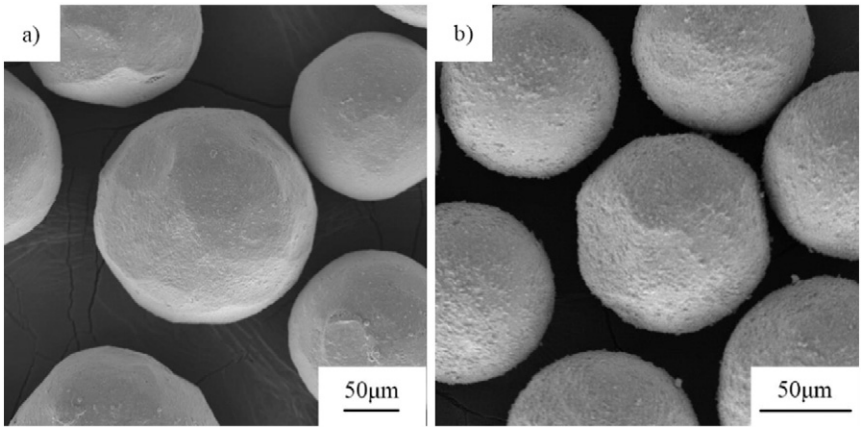

Fig. 2. SEM images of the (a) Ti6Al4V powders and (b) mixed powders after low energy ball milling.

composites were studied by SEM in detail. Fig. 4(a) and (b) shows the microstructure of Ti6Al4V alloys along cross section (CS) and longitudinal section (LS), respectively. It is not surprising to find that the widmanstätten microstructure transferred to typical basketweave microstructure after deformation because the extrusion process was carried out above β transus temperature followed by a proper cooling speed. In addition, the microstructure of the as-extruded Ti6Al4V alloys along the two sections was discovered to be similar but not totally the same with each other because the grains along cross section were pressed while the ones along longitudinal section were elongated during extrusion process.

Fig. 4(c) and (d) shows the microstructure of the TiBw/Ti6Al4V composites along cross section and longitudinal section, respectively. Compared with that of the as-sintered composites, the lamellar microstructure did keep unchanged but the network distribution of TiBw reinforcements was elongated along longitudinal section. At a higher level, this inhomogeneous distribution is similar to column microstructure, i.e., the Ti6Al4V matrix particle with column morphology and the TiBw reinforcement distributed around the column matrix particle [21]. Similar column microstructure is also obtained to improve mechanical properties in other work [10]. At last, to evaluate the difference between the as-extruded Ti6Al4V alloys and TiBw/Ti6Al4V composites, a number of grains (α-phase) along different sections was studied, the lamellar length and width was measured, as shown in Table 1. It can be concluded from the table that the as-extruded Ti6Al4V alloys had a large aspect ratio along two sections. This microstructure was

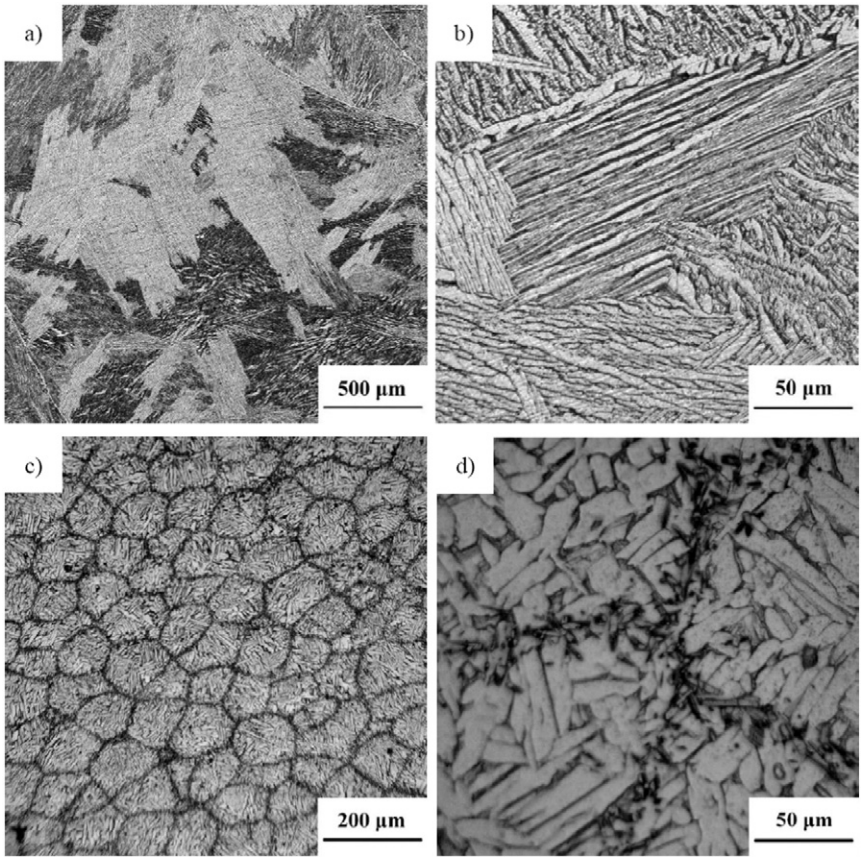

Fig. 3. Morphologies of the as-sintered (a) Ti6Al4V alloys with typical widmanstätten microstructure and (b) the feather-like microstructure at a high magnification, (c) TiBw/Ti6Al4V composites showing the novel network microstructure and (d) the morphology of different phases at high magnification.

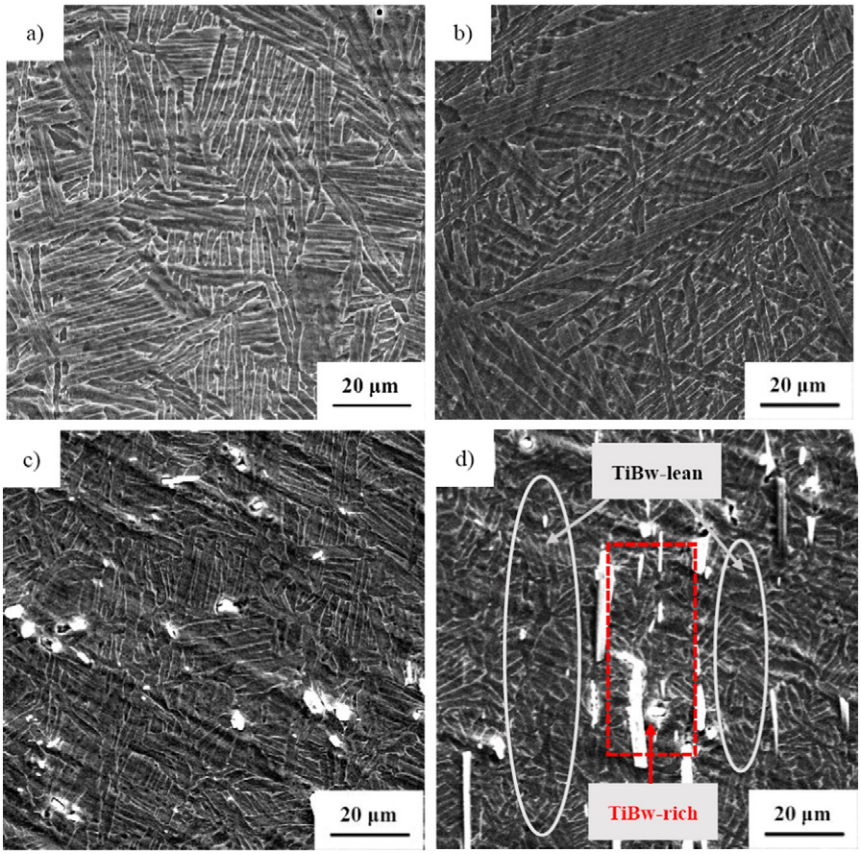

Fig. 4. Morphologies of the as-extruded (a) Ti6Al4V alloys along cross section and (b) longitudinal section, showing the basketweave microstructure, (c) TiBw/Ti6Al4V composites along cross section and (d) longitudinal section, showing the inhomogeneous distribution of the TiBw reinforcements.

considered to be unfavorable for the superplastic deformation compared with the fine and equiaxed grains. However, the aspect ratio of as-extruded TiBw/Ti6Al4V composites was much smaller than that of alloys along both of the two sections. This phenomenon might be accounted by two factors. Firstly, the ellipsoid distribution of TiBw reinforcements restrained the grain coarsen [23,24]. Secondly, the TiBw acted as nucleation sites for recrystallization due to the high density of dislocation around reinforcements during deformation [25]. These two factors led to a distinct decrease in aspect ratio, especially along the longitudinal section, were considered to be beneficial for superplastic deformation.

3.2. Superplastic tensile behaviors

3.2.1. The stress–strain curves

The high temperature tensile tests were carried out to study the superplastic deformation behaviors of the as-extruded Ti6Al4V alloys, and the engineering stress-engineering strain curves were displayed in Fig. 5. As can be seen in the figures, the stress climbed up to its peak which denoted the beginning of plastic deformation at a small strain about 15%, and then transferred to steady-state flow stage in which the true stress changed slowly. However, the as-extruded Ti6Al4V alloys did not acquire large elongations at 900 °C or 925 °C, no more than 200% at all the strain rates, which indicated weak resistance to necking tendency during plastic deformation at low temperature. It was also proved by the macro morphology of the tensile specimen after test that the fracture occurred at the necking position and formed needle-like shape. With the increasing deformation temperatures, the plastic deformation abilities of the as-extruded Ti6Al4V alloys improved, especially at low strain rate. The as-extruded Ti6Al4V alloys acquired its largest elongation of 304% at 950 °C with the strain rate of 0.000316/s, and 296% at 975 °C with the strain rate of 0.001/s, which achieve superplastic deformation.

Compared with other reports on the superplastic deformation behaviors of Ti6Al4V alloys with equiaxed microstructure and fine grain size [26–28], the elongations obtained in this study were much lower, which could be accounted by the inappropriate microstructure which has been observed in the previous section. The basketweave microstructure with a large aspect ratio was unfavorable for plastic deformation because the grain rotation was limited when compared to the equiaxed microstructure. In addition, powder sintering process before extrusion deformation maybe accompanied by harmful factors such as oxygen absorbing and grain coarsening [8], which are negative to plastic deformation of the prepared alloys. Therefore, the highest elongation of 300% should be reasonable for the prepared Ti6Al4V alloys. In summary, the titanium alloys with basketweave microstructure fabricated by powder metallurgy followed by extrusion deformation just exhibit low superplasticity.

Fig. 6 shows the true stress–strain curves of the as-extruded TiBw/Ti6Al4V composites. It can be seen from the figures that the elongations of the composites were apparently improved when compared with those of the Ti6Al4V alloys, especially at low temperature. For example, at 900 °C, the elongations were measured to be 210%, 320% and 150% at the strain rates of 0.00316/s, 0.001/s and 0.000316/s, respectively.

Table 1
The lamellar parameters of the as-extruded Ti6Al4V alloys and TiBw/Ti6Al4V composites along different sections.

	Lamellar length (μm)	Lamellar width (μm)	Aspect ratio
$CS_{Ti6Al4V}$	24.5	1.7	14.4
$LS_{Ti6Al4V}$	48.9	1.4	34.9
$CS_{TiBw/Ti6Al4V}$	14.0	1.8	7.8
$LS_{TiBw/Ti6Al4V}$	17.2	2.1	8.2

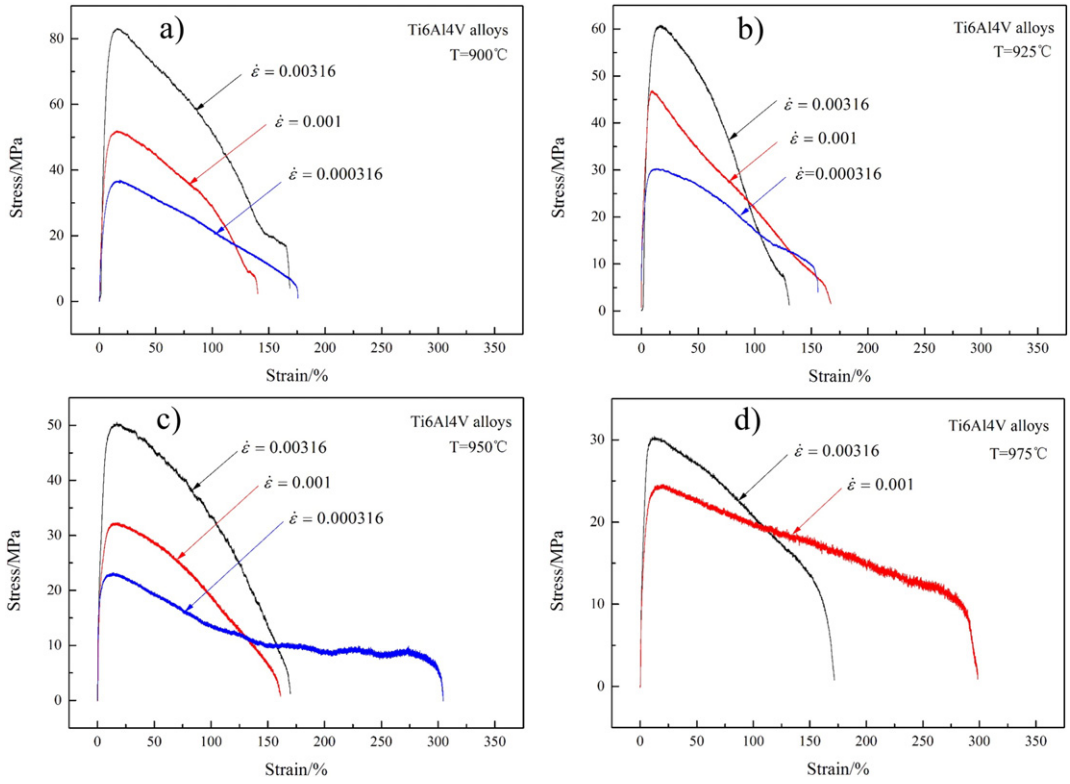

Fig. 5. The stress–strain curves of the as-extruded Ti6Al4V alloys deformed at: (a) 900 °C, (b) 925 °C, (c) 950 °C and (d) 975 °C, respectively.

When deformed at some specific parameters, an abnormal 'hardening' phenomenon that the stress increased with increasing strain occurred at large strain, which contributed to the large elongations. With increasing temperatures, the 'hardening' effect weakened. It is well known that the softening effect during high temperature deformation can be attributed to dynamic recovery and dynamic recrystallization [18]. It is certain that the softening effect is accompanied by hardening effect due to strain hardening (dislocation density growth) and grain coarsening.

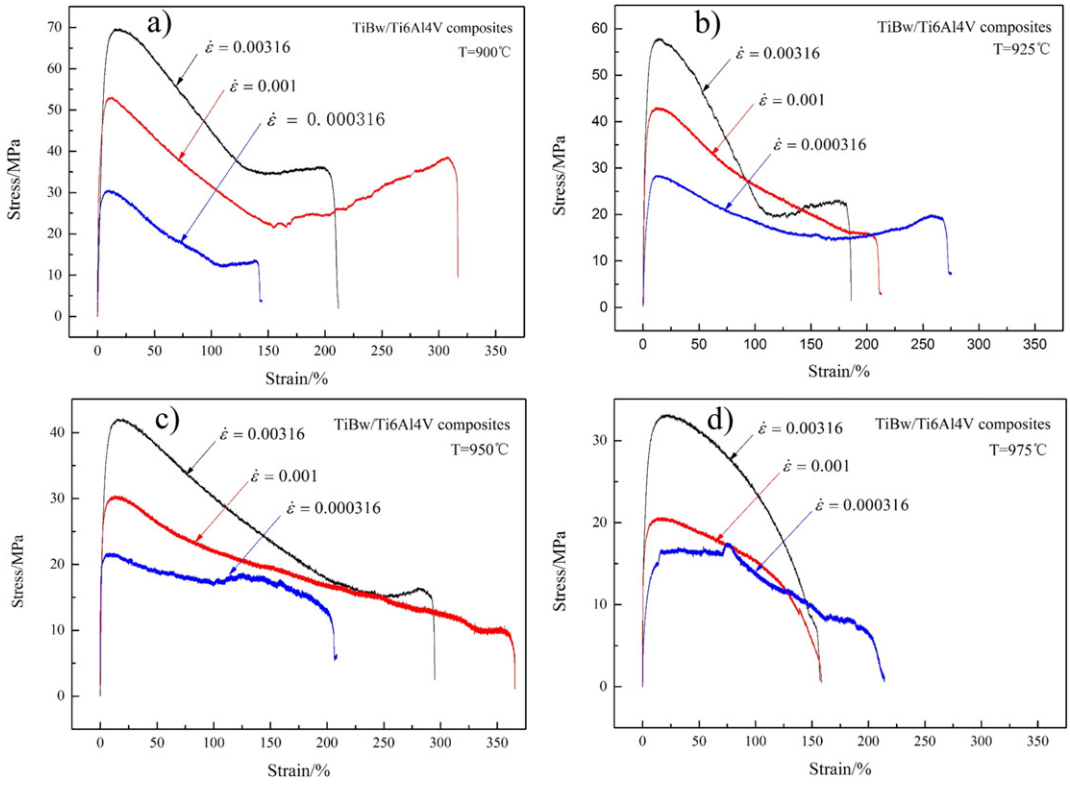

Fig. 6. The stress–strain curves of the as-extruded TiBw/Ti6Al4V composites deformed at: (a) 900 °C, (b) 925 °C, (c) 950 °C and (d) 975 °C, respectively.

At some special status, the hardening effect is probably increased to be equal to or even higher than the softening effect, which is related with inhomogeneous reinforcement, lower temperature and large strain rate. Therefore, it cannot be observed in the stress–strain curves of the alloys and the composites at higher temperatures. The abnormal 'hardening' phenomenon maybe accompanied by the phenomenon that local necking deformation is constrained and then transferred to other positions. At 925 °C, the as-extruded TiBw/Ti6Al4V composites acquired the largest elongation of 275% at the strain rate of 0.000316/s. At 950 °C, the composites acquired that of 360% at 0.001/s. It was surprising to find that the as-extruded TiBw/Ti6Al4V composites exhibit higher elongations when compared with the Ti6Al4V alloys fabricated by the same parameters. The decrease in aspect ratio analyzed in previous section could be one possible reason. Therefore, there must be some particular mechanisms functioned during the plastic deformation process of the composites. At high temperature of 975 °C, the as-extruded TiBw/Ti6Al4V composites did not acquire largest elongations at all tested strain rates, indicating that the optimal superplastic deformation temperature of the composites is lower than that of the alloys.

3.2.2. The calculation of strain rate sensitivity index and activation energy

The strain rate sensitivity index m and activation energy Q were usually used to evaluate the plastic deformation behaviors. In this study, the two values were calculated as well. The strain rate sensitivity index m stands for the resistance to necking at each temperature, and could be calculated based on the values of true stress at different strains.

However, due to the complex deformation mechanisms of the composites and avoiding the abnormal 'hardening' effect at large strain, the m values were calculated at small strains. The activation energy Q stands for the deformation mechanism at each strain rate, and could be calculated based on the values of peak stress which denoted the beginning of plastic deformation at different temperature according to [18,29]:

$$m = \frac{d\log\sigma}{d\log\dot{\varepsilon}} \tag{2}$$

$$\frac{\partial \ln\sigma}{\partial(1/T)} = \frac{mQ}{R}. \tag{3}$$

Both of the stain rate sensitivity indexes of the as-extruded Ti6Al4V alloys and TiBw/Ti6Al4V composites were calculated and listed in Fig. 7(a) and (b), respectively. It can be seen that the strain rate sensitivity index of Ti6Al4V alloys was measured to be 0.29 on average, indicating low resistance to necking tendency. The strain rate sensitivity of TiBw/Ti6Al4V composites was measured to be 0.35 on average, larger than that of the alloys, which could possibly accounted for the increase in elongations. However, the calculated m values showed weak consistency with elongations at 975 °C, which could be discovered in both Fig. 7(a) and (b). This phenomenon could be illustrated as follows: The tensile samples were kept in the test temperature for 10 min before deformation. Therefore, the microstructure might have already changed when the flow stress reached the peak value, especially at high temperature and low strain rate. The grain coarsening might increase peak stress and then weakened the consistency of the calculation results and elongations. In addition, the m values were calculated at small strain ranging from 20%–30% in this study, the results could be adopted to evaluate the necking tendency at the beginning of superplastic deformation, but might be inappropriate to be used at large strain due to the complicated superplastic deformation mechanisms behind the dual phase titanium alloys and composites with lamellar and inhomogeneous microstructure.

The calculation of activation energy Q of the as-extruded Ti6Al4V alloys and TiBw/Ti6Al4V composites was displayed in Fig. 8(a) and (b), respectively. It could be concluded from Fig. 8(a) that the activation energy of the as-extruded Ti6Al4V alloys decreased with the decreasing strain rates. At the strain rate of 0.00316/s, the activation energy was measured to be 530 kJ/mol, close to double of that at the strain rate of 0.000316/s. The decrease in activation energy suggested a change in deformation mechanisms. At higher strain rate, volume diffusion was deduced to be the major coordination mechanism during superplastic deformation process based on the large value of activation energy. However, with the decreasing strain rates, the activation energy was half of that at high strain rate, close to the value of grain boundary diffusion, which indicated that the grain boundary sliding became the superior coordination mechanism. Fig. 8(b) shows the activation energy of the as-extruded TiBw/Ti6Al4V composites. It can be seen that the values of activation energy at different strain rates were close to each other, and measured to be 352 kJ/mol on average. Compared with that of Ti6Al4V alloys, the as-extruded TiBw/Ti6Al4V composites had a smaller activation energy which suggests lower resistance to superplastic tensile deformation. Moreover, this also indicated that the grain boundary sliding might be the major coordination mechanism, possibly attributed to the smaller aspect ratio of lamellar microstructure [30]. However, due to the calculation based on the values of peak stress, the activation energy was suitable for evaluating the superplastic deformation mechanism at small strain.

3.3. Superplastic deformation mechanisms

3.3.1. Microstructure evolution

A preliminary conclusion could be drawn based on the stress–strain curves that the volume diffusion was the major coordination mechanism for the as-extruded Ti6Al4V alloys, which indicated that phase movement and dislocation motion played a significant role in superplastic deformation process of Ti6Al4V alloys with basketweave microstructure. However, the superplastic tensile behaviors of the as-extruded TiBw/Ti6Al4V composites were different with that of Ti6Al4V alloys, especially at large strains. Therefore, a typical specimen

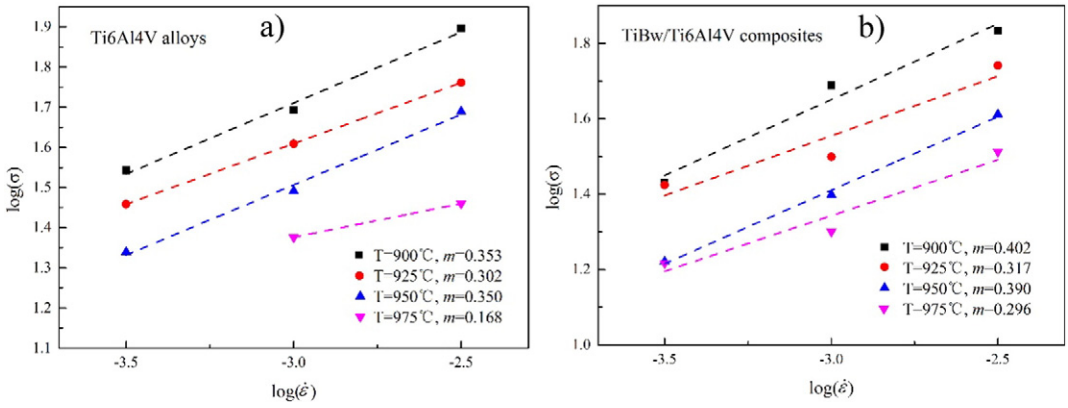

Fig. 7. Calculation of the strain rate sensitivity index of the as-extruded (a) Ti6Al4V alloys and (b) TiBw/Ti6Al4V composites.

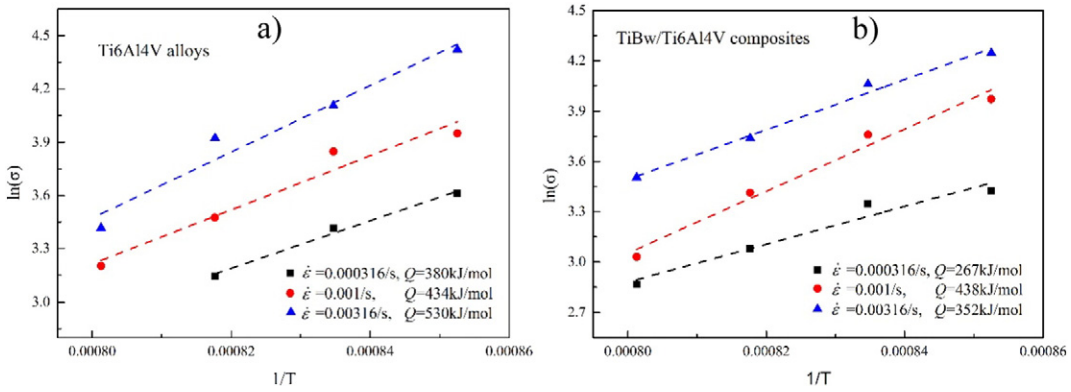

Fig. 8. Calculation of the activation energy of the as-extruded (a) Ti6Al4V alloys and (b) TiBw/Ti6Al4V composites.

with the largest elongation of 360% was adopted in this study to research the microstructure evolution of the composites during superplastic tensile test by observing the morphology at different positions. In addition, the specimen of the as-extruded Ti6Al4V alloys deformed at the same parameters was studied as well to distinguish the function mechanism of TiBw reinforcements during superplastic deformation.

The tensile specimen of the as-extruded Ti6Al4V alloys deformed at 950 °C and 0.001/s fractured at the elongation of 155%, suggesting a high necking tendency, which formed the needle-like shape of fracture, showed in Fig. 9. To study the microstructure evolution, the morphology at different strains was observed based on the nonuniform deformation at different positions: the grip area is held by the chuck and the strain equal to 0 while the true strain of necking area is much larger than the final elongation. In this study, four areas were selected and the morphology of each area was shown in Fig 9(a)–(d), respectively. It could be observed from the Fig. 9(a) that the basketweave microstructure kept unchanged and the aspect ratio of the lamellar α-phase did not decrease in the grip area. Therefore, only static recovery and grain coarsening functioned in the grip area during tensile tests carried out below the β transus temperature of Ti6Al4V alloys. Fig. 9(b) shows the morphology of the near-grip area with a small strain. In this area, the basketweave microstructure could still be observed but the aspect ratio of the lamellar α-phase apparently decreased. Compared with the microstructure in the grip area, the difference between the two areas should be attributed to the small strain deformation at the same temperature for the same time. In addition, a group of lamella shared the same orientation in this area which indicated that the lamellar α-phase might slide by group, because the microstructure with a large

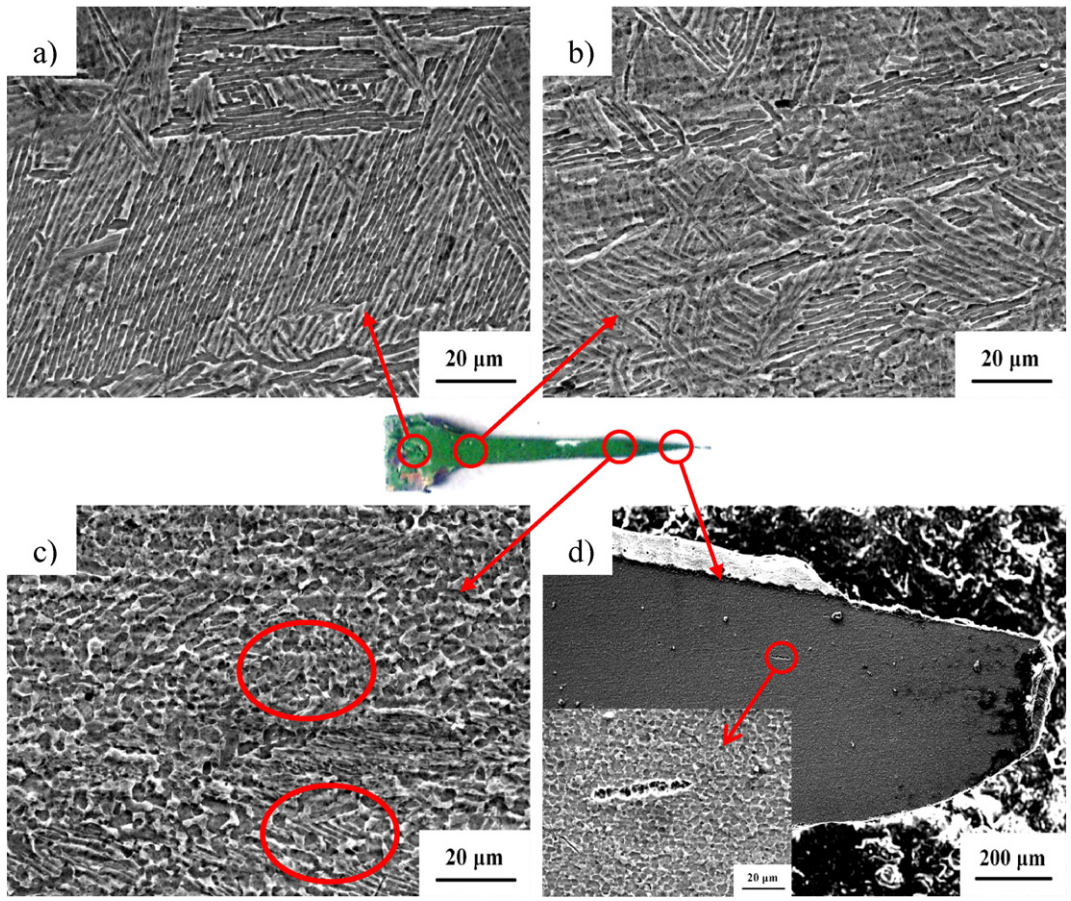

Fig. 9. The microstructure evolution of the as-extruded Ti6Al4V alloys during tensile tests: (a) grip area, (b) near grip area, (c) near tip area and (d) tip area.

aspect ratio was unfavorable for plastic deformation, especially for the grain rotation. Fig. 9(c) shows the morphology of the near-tip area with a large strain. As can be seen, a part of the primary lamellar α-phase has transformed to equiaxed microstructure, and the equiaxed (the circle 1 marked in the figure) and lamellar (the circle 2 marked in the figure) α-phase coexisted in this area. However, with the rising fraction of transformed equiaxed α-phase, this area became more suitable for plastic deformation than the areas with lamellar microstructure, due to the effect of coordination mechanisms including grain boundary sliding and grain rotation.

When it comes to the tip area showed in Fig. 9(d), all of the primary lamellar α-phase has transformed to equiaxed microstructure with fine grain size. Based on the calculation results in previous section, the activation energy of grain boundary diffusion was nearly half that of volume diffusion, suggested a reducing in flow stress with the decreasing of lamellar aspect ratio. Therefore, the engineering flow stress in this area was smaller than the true stress, led to an increasing in strain rate. However, necking in this area could not be transmitted to other positions with unfavorable microstructure. In addition, a small volume fraction of voids could be observed only in the tip area, and found to distribute along the tensile direction.

Fig. 10 shows the microstructure evolution of the as-extruded TiBw/Ti6Al4V composites deformed at 950 °C with a strain rate of 0.001/s, and fractured at the elongation of 360%. Similar to the Ti6Al4V alloys, four areas were studied to distinguish the microstructure evolution of the composites during superplastic deformation. It can be seen from the Fig. 10(a) that both the distribution of TiBw and lamellar microstructure of α-phase kept the same with those before superplastic deformation, suggesting that only static recovery and grain coarsen functioned in the grip area [31]. However, in the near grip area with small strain showed in Fig. 10(b), the microstructure was totally different from that in the grip area. The primary lamellar α phase has already transformed to the equiaxed ones (the dark phase in the figure) with a grain size of 12 μm on average. In addition, the volume fraction of β phase (the light phase in the figure) in this area increased obviously compared with that in the grip area. When it came to the near tip area as shown in Fig. 10(c), all the lamella microstructure had transferred to the equiaxed grains. In addition, the grain size of the equiaxed α phase further was slightly decreased compared with that near grip area, and correspondingly the volume fraction of β phase was increased to be about 50%. The phase transformation is considered to be favorable for the superplastic deformation due to that the process is accompanied with volume augmenting effect. However, the volume fraction of β phase in the as-extruded Ti6Al4V alloys after superplastic tensile test was much smaller, though deformed at the same temperature and strain rate, suggesting that the phase transformation was not the major coordination mechanism in the as-extruded Ti6Al4V alloys.

Therefore, the phase transformation companied with the grain globalization process was induced by plastic deformation, which suggested that the dynamic recrystallization might be the major coordination mechanism for the as-extruded TiBw/Ti6Al4V composites. Fig. 10(d) shows the morphology of the tip area. It can be seen that the volume fraction of voids increased in this area and mainly distributed along the tensile direction next to the TiBw reinforcements. On the one hand, the reinforcements acted to pin the grain boundary and might be unbeneficial for the grain boundary sliding. However, when compared with that of the as-extruded Ti6Al4V alloys showed in Fig. 9(d), it was interesting to discover that the volume fraction of voids in the

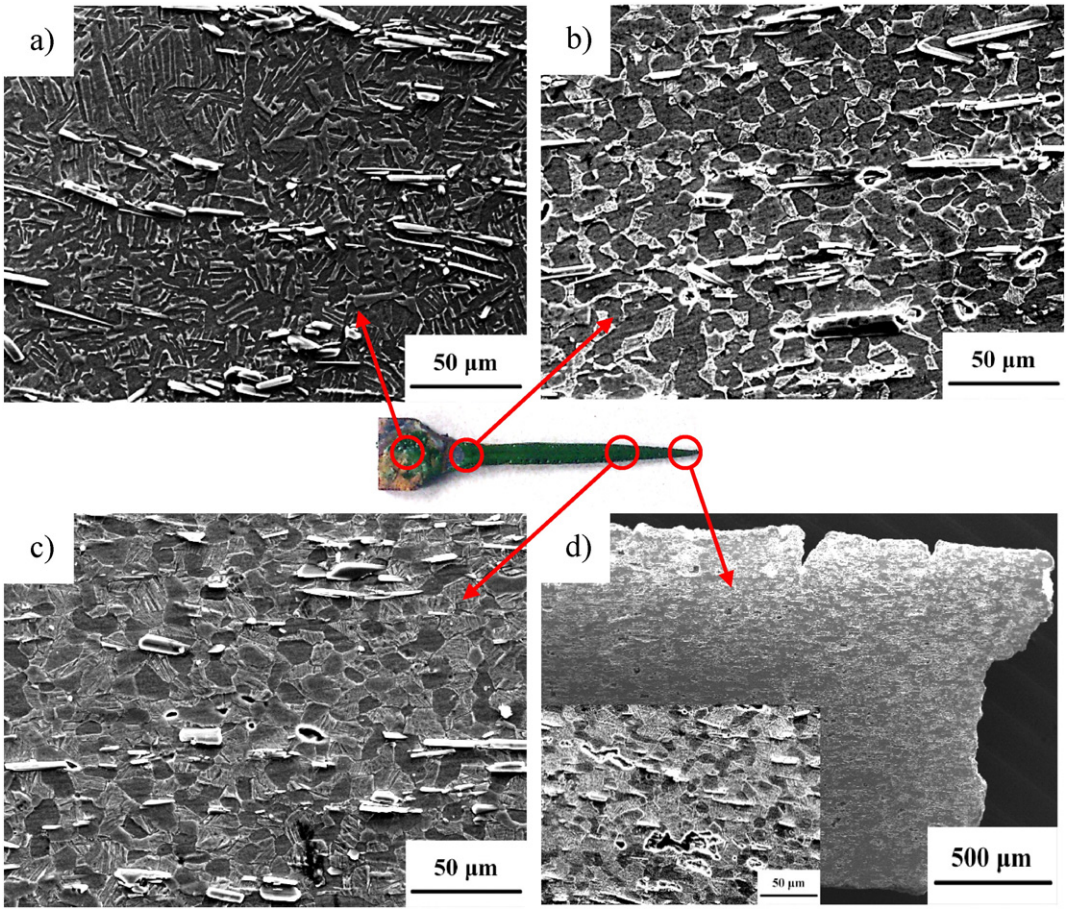

Fig. 10. The microstructure evolution of the as-extruded TiBw/Ti6Al4V composites during tensile tests: (a) grip area, (b) near grip area, (c) near tip area and (d) tip area.

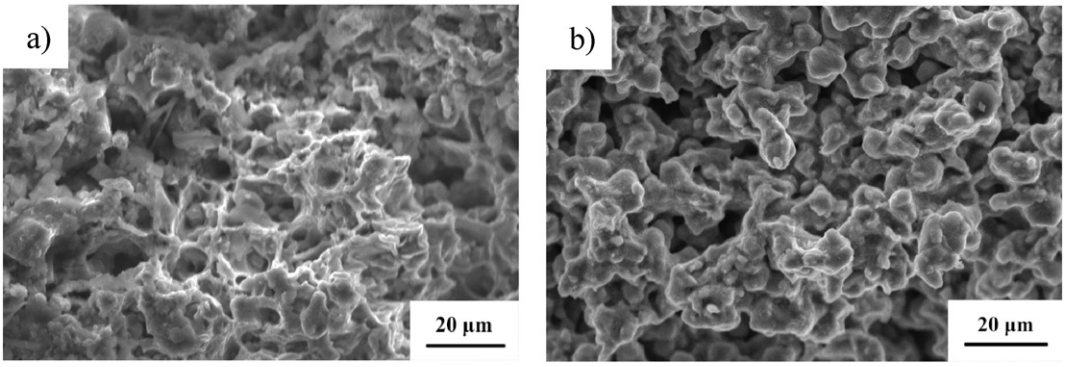

Fig. 11. The fracture morphology of superplastic tensile specimens of the as-extruded (a) Ti6Al4V alloys and (b) TiBw/Ti6Al4V composites deformed at 950 °C and 0.001/s.

composites was much higher. When the voids formed during the superplastic deformation process, the flow stress of the nearby grains increased, as well as the true strain rate, which was similar to the process of local necking. According to the previous analysis, the local necking in the tip area of the as-extruded Ti6Al4V alloys could not be transmitted to other positions with unfavorable microstructure, thereby the volume fraction of voids in the alloys was small and the cracks formed on voids or grain boundary. However, when it comes to the as-extruded TiBw/Ti6Al4V composites, the reinforcements constrained the deformation and helped to prevent crack propagation and postpone the failure of specimen during superplastic tensile test, leading to the strong resistance to necking tendency and large volume fraction of voids. In summary, the TiBw reinforcements could not only help to constrain deformation but also keep the grain from coarsening and cracks from propagation, accounted for the weak necking tendency of the as-extruded TiBw/Ti6Al4V composites. What's more, the TiBw reinforcements contributed to recrystallization by promoting the density of piled-up dislocation during deformation process. Contrast to the alloys, the as-extruded TiBw/Ti6Al4V composites formed the equiaxed microstructure with a small aspect ratio at small strain. Therefore, the flow stresses at different positions were similar and the necking could be effectively constrained and then transmitted to other positions, promoting high elongations of the composites at proper deformation parameters.

3.3.2. Fracture morphology

A comparative study on fracture morphology of the TiBw/Ti6Al4V composites and Ti6Al4V alloys was carried out to reveal the function mechanism of TiBw reinforcements. Fig. 11(a) shows the fracture morphology of the Ti6Al4V alloys, and the typical dimple surfaces could be observed. However, voids in this study were not formed by the second phase particles but formed on the grain boundary by during superplastic deformation process in the tip area of the tensile specimen which has been observed in the Fig. 9(d). Afterwards, the flow stress of the positions with voids decreased but the necking could not be transferred to other positions with unfavorable microstructure. Therefore, the true strain rate at the necking position was much larger and then formed the dimple surfaces, a typical fracture surface of the ductile alloys when deformed at higher strain rates. However, the fracture morphology of the TiBw/Ti6Al4V composites was totally distinguished from that of Ti6Al4V alloys. The intact grain appearance could be observed in Fig. 10(b). Due to that the deformation was carried out at high temperature, the grain boundary weakened and the strength decreased. Grain boundary sliding and grain rotation were two major coordination mechanisms of the Ti6Al4V alloys and TiBw/Ti6Al4V composites with equiaxed microstructure at high elongation. However, necking in the TiBw/Ti6Al4V alloys could be restrained by transferring to other positions with similar microstructure, promoting the grain boundary sliding and then led to the intact grain appearance.

4. Conclusions

(1) The as-extruded TiBw/Ti6Al4V composites with inhomogeneous microstructure exhibited higher superplasticity/tensile elongation than the Ti6Al4V alloys fabricated by the same powder metallurgy and extrusion deformation.
(2) The strain rate sensitivity index m of the prepared TiBw/Ti6Al4V composites is higher than that of the Ti6Al4V alloys, which suggests higher ability constraining necking deformation, while the activation energy Q is smaller suggesting lower resistance by the major coordination mechanism of grain boundary sliding.
(3) The as-extruded Ti6Al4V alloys failed with needle-like fracture morphology, which can be attributed to serious necking deformation due to lamellar microstructure, grain coarsening and reinforcement absence.
(4) The high elongation of the as-extruded TiBw/Ti6Al4V composites can be contributed to inhomogeneously distributed TiBw reinforcement, globalization process and dynamic recrystallization which are beneficial to constraining necking deformation, the grain boundary sliding and grain rotation.

Acknowledgments

This work is financially supported by the National Natural Science Foundation of China (NSFC) under Grant Nos. 51471063 and 51271064, the High Technology Research and Development Program of China (863) under Grant No. 2013AA031202, the Fundamental Research Funds for the Central Universities (Grant No. HIT.BRETIII.201401) and China Postdoctoral Science Foundation funded project (Grant No. LBH-Q15037).

References

[1] S.K. Choi, M. Chandrasekaran, M.J. Brabers, J. Mater. Sci. 25 (1990) 1957–1964.
[2] S.C. Tjong, Y.W. Mai, Compos. Sci. Technol. 68 (2008) 583–601.
[3] L. Geng, L.J. Huang, Acta Metall. Sin.-Engl. 27 (2014) 787–797.
[4] M.M. Wang, W.J. Lu, J.N. Qin, D. Zhang, B. Ji, F. Zhu, Scr. Mater. 54 (2006) 1955–1959.
[5] L. Xiao, W.J. Lu, Z.F. Yang, J.N. Qin, Z. Di, M.M. Wang, F. Zhu, B. Ji, Mater. Sci. Eng. A 491 (2008) 192–198.
[6] Z.Y. Ma, S.C. Tjong, L. Gen, Scr. Mater. 42 (2000) 367–373.
[7] Y. Yu, W. Zhang, W. Dong, X. Han, C. Pei, X. Jiao, Y. Feng, Mater. Des. 73 (2015) 1–9.
[8] L.J. Huang, L. Geng, H.X. Peng, Prog. Mater. Sci. 71 (2015) 93–168.
[9] L.J. Huang, L. Geng, H.X. Peng, J. Zhang, Scr. Mater. 64 (2011) 844–847.
[10] W.C. Zhang, M.M. Wang, W.Z. Chen, Y.J. Feng, Y. Yu, Mater. Des. 88 (2015) 471–477.
[11] A.H. Chokshi, A.K. Mukherjee, T.G. Langdon, Mater. Sci. Eng. R 10 (1993) 237–274.
[12] A.K. Mukherjee, R.S. Mishra, Superplasticity in intermetallics, in: A.H. Chokshi (Ed.), Superplasticity in Advanced Materials — Icsam-97, Trans Tech Publications Ltd, Stafa-Zurich 1997, pp. 609–617.
[13] T.G. Nieh, J. Wadsworth, Int. Mater. Rev. 44 (1999) 59–75.
[14] G. Wang, M.W. Fu, J. Materials, Processing and Technology 192 (2007) 555–560.
[15] X.F. Xu, J.G. Zhang, C.F. Liu, G.C. Wang, Z.H. Yun, J. Materials Engineering, Performance 23 (2014) 187–192.
[16] V. Sinha, R. Srinivasan, S. Tamirisakandala, D.B. Miracle, Mater. Sci. Eng. A 539 (2012) 7–12.

[17] J. Lu, J. Qin, Y. Chen, Z. Zhang, W. Lu, D. Zhang, Alloys and Compounds 490 (2010) 118–123.
[18] L.J. Huang, Y.Z. Zhang, B.X. Liu, X.Q. Song, L. Geng, L.Z. Wu, Mater. Sci. Eng. A 581 (2013) 128–132.
[19] T.S. Srivatsan, W.O. Soboyejo, R.J. Lederich, Compos. Part A 28 (1997) 365–376.
[20] Y. Yu, W. Zhang, W. Dong, J. Yang, Mater. Sci. Eng. A 638 (2015) 38–45.
[21] H.K.S. Rahoma, X.P. Wang, F.T. Kong, Y.Y. Chen, J.C. Han, M. Derradji, Mater. Des. 87 (2015) 488–494.
[22] M.Y. Koo, J.S. Park, M.K. Park, K.T. Kim, S.H. Hong, Scr. Mater. 66 (2012) 487–490.
[23] K.S. Munir, Y. Li, D. Liang, M. Qian, W. Xu, C. Wen, Mater. Des. 88 (2015) 138–148.
[24] B. Wang, L.J. Huang, L. Geng, X.D. Rong, B.X. Liu, Mater. Des. 85 (2015) 679–686.
[25] M. Karimi, M.R. Toroghinejad, K. Farmanesh, Mater. Des. 65 (2015) 34–41.
[26] J.P. Escobedo, S.N. Patankar, D.P. Field, F.H. Froes, Mater. Technol. 21 (2006) 84–87.
[27] N.S. Reddy, Y.H. Lee, J.H. Kim, C.S. Lee, Met. Mater. Int. 14 (2008) 213–221.
[28] H. Matsumoto, V. Velay, A. Chiba, Mater. Des. 66 (2015) 611–617.
[29] J.W. Edington, K.N. Melton, C.P. Cutler, Prog. Mater. Sci. 21 (1976) 61–170.
[30] C.J. Lu, L.J. Huang, L. Geng, B. Kaveendran, Z.Z. Zheng, J. Zhang, Mater. Charact. 104 (2015) 139–148.
[31] X. Guo, L. Wang, M. Wang, J. Qin, D. Zhang, W. Lu, Acta Mater. 60 (2012) 2656–2667.